A universal strategy to fabricate metal sulfides@carbon fibers as freestanding and flexible anodes for high performance lithium/sodium storage

Journal:	*ACS Applied Energy Materials*
Manuscript ID	ae-2019-00669k.R1
Manuscript Type:	Article
Date Submitted by the Author:	10-May-2019
Complete List of Authors:	Du, Ting; Zhejiang University Zhu, Hang; Zhejiang University Xu, Ben; Northumbria University at Newcastle upon Tyne, Mechanical Engineering Liang, Chu; Zhejiang University of Technology, College of Materials Science and Engineering Yan, Mi; Zhejiang University Jiang, Yinzhu; Universitat Bielefeld, Dept. of Chem.

A universal strategy to fabricate metal sulfides@carbon fibers as freestanding and flexible anodes for high performance lithium/sodium storage

*Ting Du,[a] Hang Zhu,[a] Ben Bin Xu,[b] Chu Liang,[c] Mi Yan,[a] Yinzhu Jiang [a,d]**

[a]State Key Laboratory of Silicon Materials, Key Laboratory of Novel Materials for Information Technology of Zhejiang Province and School of Materials Science and Engineering, Zhejiang University, Hangzhou, Zhejiang 310027, PR China

[b]Smart Materials and Surfaces Lab, Mechanical Engineering, Faculty of Engineering and Environment, Northumbria University, Newcastle upon Tyne NE1 8ST , UK

[c]College of Materials Science and Engineering, Zhejiang University of Technology, Hangzhou, Zhejiang 310014, PR China

[d]State Key Laboratory of Structural Chemistry, Fujian Institute of Research on the Structure of Matter, Chinese Academy of Science, Fuzhou, Fujian 350002, PR China

KEYWORDS

flexible electrode; freestanding; metal sulfide; electrospinning; L-cysteine

ABSTRACT

The future trend toward flexible electronics demands for flexible power sources using rechargeable batteries, where freestanding and flexible electrodes are of critical importance. The utilization of high capacity anode materials like metal sulfides in flexible batteries is highly desirable for the miniaturization of electronic devices, nevertheless very challenging in the fabrication of electrode that is freestanding and flexible. Herein, a universal electrospinning strategy to fabricate freestanding and flexible metal sulfides@carbon electrodes is proposed based on the formation of chelate complexes between L-cysteine and metal cations. Taking SnS as a model material, flexible fiber electrodes are realized with SnS nanoparticles well embedded in the continuous and interwoven carbon fibers. As freestanding electrodes for lithium and sodium storage, high capacity, good rate capability and excellent cycling stability are simultaneously achieved. Such strategy is also successfully extended to the fabrication of Ni_3S_2/C fibers and Fe_7S_8/C fibers, suggesting the universality in fabricating freestanding and flexible high capacity electrodes.

1. Introduction

Rechargeable batteries have successfully powered the humankinds' modern life, ranging from portable electronics, electric vehicles, to the emerging large-scale energy storage system. Lithium ion batteries (LIBs) are amongst the best battery technology which possesses the advantages of high energy density, no memory effect and long service life.[1-5] However, the resource limitation of lithium in the earth's crust has become one of main obstacles to satisfy the rapid growth of energy storage market. Operating under the same working-principle as LIBs, sodium ion batteries (SIBs) recaptured the attention to enrich the energy storage technology due to its similar chemistry to Li and high natural abundance.[6-9] Recently, rechargeable batteries like

LIBs and SIBs are also extending their usage as power sources in the area of flexible electronics, where light-weight and flexible electrodes are one of key factors to meet the requirements.[10-13]

Graphite-based materials have been applied as anodes for LIBs in the past decades. However, their limited theoretical specific capacity (372 mAh g^{-1}) has obstructed the light-weighting of the electrode for LIBs.[14-16] Furthermore, graphite has failed for sodium storage in traditional EC/DEC electrolyte system due to the superior difficulty in forming staged Na-intercalation compounds.[17-21] Transition metal sulfides, TMS, have emerged as a competitive anodes materials for SIBs. Compared with transition metal oxides for LIBs, TMS show a more competitive advantage due to its high electric conductivity, which is caused by the weaker M-S bond than M-O bond.[22-23] Furthermore, metal sulfides undergoing conversion and/or alloying reactions upon lithium/sodium storage can deliver high theoretical capacity, which offer the huge possibility to be explored as light-weight and flexible electrodes.[23-27] Electrospinning has been demonstrated as a cheap, versatile and scalable technique for the fabrication of flexible electrode materials, such as metal-oxide/carbon [28-29] and metal/carbon composite electrodes.[30] However, when it comes to the metal-sulfides/carbon composites, successful application is quite rare yet. The introduction of sulfur in the previous reports is generally realized by additional sulfuration process, such as annealing under H_2S atmosphere [31-32] or with sulfur gas,[33] during which the flexibility is unavoidably destroyed. Employing sulfur-containing precursors during electrospinning also works, but choosing suitable precursor is tough and further limits its universality.[34] Thus, it is highly desirable to develop a universal strategy with no need of additional sulfuration process for fabricating flexible metal-sulfides/carbon composite electrodes by electrospinning for both lithium and sodium storage.

Herein, a facile and universal strategy via a coaxial electrospinning method is proposed for the fabrication of freestanding and flexible metal sulfides@carbon fiber electrodes. The in-situ formation of metal sulfides is enabled through the formation of M-S bonds between metal cations and R-SH of L-cysteine in the precursor solution. The flexible composites consist of metal sulfide nanoparticles well embedded in the amorphous carbon matrix, which exhibit high capacity, good rate capability and long cycle life as freestanding electrodes both for lithium and sodium storage.

2. Experimental Section

2.1. Materials synthesis. SnS/C fiber composites were prepared via a coaxial electrospinning method followed by a post-treatment process, which is designated as Coa-SnS/C. 0.6 g Polyacrylonitrile (PAN, average MW = 150 000) and 0.5 g Polyvinylpyrrolidone (PVP, average MW = 1300 000) were dissolved in 7 and 5 mL dimethylformamide (DMF) respectively. After stirring for 2 hours, $SnCl_2$ (0.6 M) and L-cysteine (0.66 M) were added into the above solution containing PVP. Keeping stirring for another 10 hours, the obtained viscous suspensions were separately loaded into two plastic syringes connected to a coaxial spinneret. The spinneret was assembled by two coaxial stainless steel capillaries. The inner diameters of the outer and inner steel capillaries were 0.4 and 0.9 mm, respectively. In the subsequent electrospinning process, the solution containing PVP was fed into the inner capillary while the solution containing PAN into the outer capillary at a constant flow rate of 0.5 mL h^{-1}. The spinneret was connected to a high-voltage power supply and a voltage of 12 kV was applied to initiate the electrospinning process. The distance was set to be ~20 cm from the spinneret to the fiber collector. The electrospun fibers were then stabilized at 200 and 250 ºC each for an hour in air with a heating

rate of 2 ºC min^{-1}. Eventually, Coa-SnS/C were obtained after annealing at 650 ºC for 4 h under Ar atmosphere with a heating rate of 5 ºC min^{-1}. Moreover, we changed the corresponding metal precursor from $SnCl_2$, to $NiCl_2$ and $FeCl_2$ with the same concentration to fabricate Ni_3S_2/C fibers and Fe_7S_8/C fibers, respectively.

For comparison, a single axial electrospinning method was applied for the preparation of Uni-SnS/C using the same solution of core layer of Coa-SnS/C. The experimental parameters in the processes of electrospinning, pre-oxidation and annealing coincide with those in coaxial electrospinning method, except for a single axial electrospinning spinneret with a diameter of 0.4 mm.

2.2. Characterization. Fourier transform infrared spectroscopy (FT-IR, SGE/Agilent 6890/Nicolet 5700) were obtained within 500 ~ 4000 cm^{-1}. Notably, the liquid test samples were the same as the corresponding precursor solutions of core layer of Coa-SnS/C, Ni_3S_2/C and Fe_7S_8/C fibers without adding PVP. The morphology of the composites was characterized by scanning electron microscopy (SEM, Hitachi S-4800), and transmission electron microscope (TEM, JEOL 2100F). The composition and crystal structure were characterized by X-ray diffraction (X Pert PRO) in a 2θ range of 10~80º. Thermal gravimetric analysis (TGA) was performed on a Pyris 1 TGA thermal analyzer in air at a heating rate of 10 ºC min^{-1}.

2.3. Electrochemical measurements. The Coa-SnS/C, Uni-SnS/C, Ni_3S_2/C and Fe_7S_8/C fiber composites were directly used as electrodes after being cut into disks without mechanical milling or slurry coating. The loading weight of the electrodes is around 1 mg cm^{-2} and the area of electrode is 1 cm^2. For the assembly of the half cells, metallic lithium (sodium for SIBs) disks were employed as counter and reference electrodes. The electrolyte for LIBs contained 1 M

$LiPF_6$ in the solvent of ethylene carbonate (EC) and diethyl carbonate (DEC) (1:1 by volume), while the electrolyte for SIBs contained 1 M $NaClO_4$ in the solvent of EC, DEC and propylene carbonate (PC) (4:4:2 by volume). Besides, 5% fluoroethylene carbonate (FEC) was added into the above both electrolytes. Afterwards, coin-type cells (CR2025) were assembled in an argon-filled glovebox when the water and oxygen concentrations both were lower than 0.1 ppm. The galvanostatic charge/discharge tests were performed with a Neware BTS-5 battery test system. Cyclic voltammetry (CV) in a voltage range between 2.50 and 0.01 V vs Li/Li^+ (Na/Na^+, SIBs) and electrochemical impedance spectroscopy (EIS) were carried out on a CHI660C electrochemistry workstation.

3. Results and Discussion

A facile one-step fabrication procedure of metal sulfides@carbon fibers via a coaxial electrospinning method is illustrated in **Figure 1**a. PVP/metal salt/L-cysteine and PAN are chosen as the precursors of the core and shell layer separately. L-cysteine possesses three different ligands, thiol group (R-SH), carboxyl group (R-COOH) and amino group ($R-NH_2$), which are expected to bond with metal ions to form chelate complex.[35-38] The key to prepare metal sulfides using electrospinning technique is the formation of bonds between metal cations and R-SH of L-cysteine. FT-IR spectroscopy was conducted to determine the bonding states between $SnCl_2$ and L-cysteine, as shown in Figure 1c. Two absorption peaks at 2552 and 942 cm^{-1}, which are attributed to characteristic peaks of the R-SH group in L-cysteine, disappear in the mixed solution of $SnCl_2$ and L-cysteine. It clearly indicates that L-cysteine is coordinated to tin (II) cation through sulfur atom.[36, 39-40] Another two peaks at 2082 and 1532 cm^{-1} of R-NH2 group are also absent in the chelate complex, representing the coordination between Sn^{2+} and

nitrogen atom.[35, 38] Furthermore, there is no significant change about the characteristic peaks of the R-COOH group with a slight shifting of one peak from 1588 to 1658 cm^{-1}, which suggests unfavorable formation of Sn-O bond.[35, 37] According to the FT-IR results, the typical molecular structure of chelate complex is illustrated as shown in Figure 1b, which is characterized by the bonding among Sn^{2+}, sulfur and nitrogen atom. Worthy of noting is that the electrospun fibers after pre-oxidation shows the similar FT-IR characteristic peaks as that in the chelate complex, demonstrating the stability of bonding states (Figure S1).[41-42] Such chelate complex in the precursor solution enables the in-situ formation of metal sulfides during electrospinning and subsequent annealing, as verified that all of the XRD peaks can be well indexed to orthorhombic SnS (JCPDS No. 75-2115) in **Figure 2**a. Furthermore, Uni-SnS/C via a single axial electrospinning method was also prepared using the same precursor of the core layer of coaxial electrospinning fibers (Coa-SnS/C). No obvious difference is found between their XRD patterns,

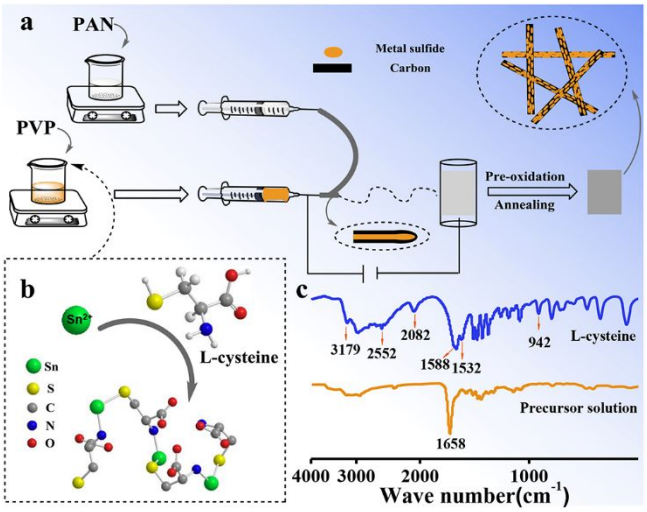

Figure 1. (a) Schematic illustration of the fabrication procedure of metal sulfides@carbon fibers via a coaxial electrospinning method; (b) The proposed structure of chelate complex between L-cysteine and metal cations; (c) The FT-IR spectra of L-cysteine and the mixed solution of $SnCl_2$ and L-cysteine (precursor solution without adding PVP) within 500 ~ 4000cm^{-1}.

revealing that it is the chelate complex rather than the electrospinning method matters in the formation of metal sulfides.

Both Uni-SnS/C and Coa-SnS/C show smooth fibrous morphologies before annealing, as shown in Figure S2. However, Figure 2b-c show the SEM pictures of Uni-SnS/C and Coa-SnS/C. Different from the rough morphology with lots of nanoparticles dispersed on the surface of fibers in Uni-SnS/C, Coa-SnS/C fibers exhibit quite smooth surface. Furthermore, Coa-SnS/C fibers with a narrower diameter distribution and smaller average diameter exhibit good flexibility even at a large bending angle (Figure 2d), which is indispensable for the fabrication of flexible energy storage devices. TEM analysis was further conducted to identify the refined morphology and microstructure of a single Coa-SnS/C fiber. The SnS nanoparticles are well embedded in the amorphous carbon matrix, which is due to the confinement effect of out-layer assuring the fast electron transfer and good buffering during charge/discharge.[43-45] Furthermore, amorphous structures of metal sulfides can be detected from both the XRD and TEM results, which have been verified in improving the capacity, rate capability and long-term cycling stability of LIBs and SIBs.[46] Metal-sulfides/carbon composites fabricated via such coaxial electrospinning method are freestanding when served as electrodes due to their good flexibility, meaning that neither an insulating binder nor an additional conducting agent is required. Above all, heavy current collectors (e.g. copper foil, around 7~10 mg cm^{-2}), which provide no capacity but might lead to poor contact with active materials, can be discarded to greatly improve the energy density of whole battery devices.

We further conducted detailed electrochemical analyses to explore the lithium/sodium storage performance using such freestanding Coa-SnS/C as working electrodes. CV analysis was carried out for the first three cycles at a scan rate of 0.1 mV s^{-1} in the voltage range of 0.01 to 2.5 V to

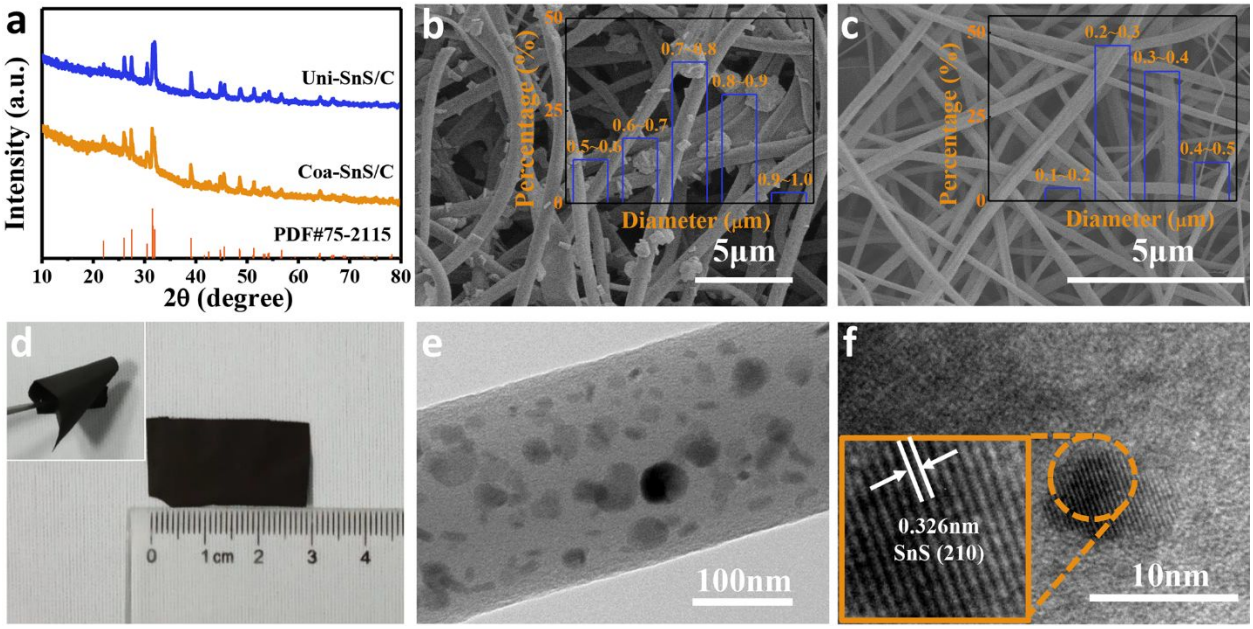

Figure 2. (a) XRD patterns of Uni-SnS/C and Coa-SnS/C. The standard reflections of SnS (JCPDS No. 75-2115) are displayed at the bottom; (b, c) SEM images of Uni-SnS/C (b) and Coa-SnS/C (c) and their corresponding diameter distribution histogram; (d) Digital photographs of Coa-SnS/C at a large bending angle; (e) TEM image of Coa-SnS/C; (f) HRTEM of a single Coa-SnS/C fiber.

clarify the electrochemical process. **Figure 3**a shows the CV curves for lithium storage. During the first cathodic scan, the distinctive reduction peak at 1.34 V is attributed to the conversion reaction of SnS to Sn and Li2S ($SnS + 2Li^+ + 2e^- = Sn + Li_2S$). The peak located at 0.35 V corresponds to the alloying reaction of Sn and Li (Sn + xLi+ + xe- = LixSn). A wide irreversible peak ranging from 0.7 V to 1.2 V reveals the formation of the solid electrolyte interphase (SEI) film, while the similar phenomenon has occurred in other previously reported Sn-based anode materials.[47-48] Subsequently, in the first anodic scan, four peaks at 0.50, 0.62, 0.80 and 1.18 V represent the multi-step Li–Sn dealloying processes and the wide peak around 2.0 V is ascribed to the reversible conversion of Sn and Li_2S into the SnS phase.[49-50]

Similar to lithium storage, the CV curves for sodium storage also present the reduction peaks corresponding to conversion and alloying reactions. In the first cathodic scan, the peak at 1.05 V is attributed to the conversion reaction of SnS to Sn and Na_2S ($SnS + 2Na^+ + 2e^- = Sn + Na_2S$). The distinctive reduction peak around 0.35 V corresponds to the alloying reaction of Sn and Na ($Sn + xNa^+ + xe^- = Na_xSn$) together with the formation of the solid electrolyte interphase (SEI) film.[51-53] Another alloying reaction peak at 0.55 V also represents the multi-step alloying process. However, the CV peaks for sodium storage are much broader and weaker than those for lithium storage, which should be largely ascribed to the sluggish kinetics resulting from the larger ionic radius (Na^+/Li^+, 0.102 nm/0.076 nm).[54] Furthermore, from the second scan onward, all the CV curves for both lithium and sodium storage are clearly overlapped, revealing excellent reversibility of Coa-SnS/C as electrodes of LIBs and SIBs.

The charge/discharge profiles of Coa-SnS/C in terms of lithium and sodium storage are depicted in Figure 3b and 3e at a current density of 50 mA g^{-1} between 0.01 and 2.5 V. The first discharge/charge capacity reach 1155.3/812.7 mAh g^{-1} for lithium storage and 500.8/327 mAh g^{-1} for sodium storage respectively, corresponding to the Coulombic efficiency (CE) of 70.3% and 65.3%. The much lower capacity of Coa-SnS/C anodes in SIBs than that in LIBs is in agreement with the broader and weaker CV peaks for sodium storage, as a consequence of the sluggish kinetics of sodium insertion and extraction.[55] The initial capacity loss mainly results from the formation of SEI layer and decomposition of electrolyte.[53] Worthy of noting is that the specific capacity values in the present work are calculated based on the total mass of the composite, which could be even higher by deducting the content of carbon, 55.2% observed from the TGA curve (Figure S3).

Figure 3c shows the superior rate performance of Coa-SnS/C anodes in LIBs. A reversible capacity of 752.1, 633.4, 556.7, 484, 389.7 and 317.9 mAh g^{-1} is achieved under the current density of 50, 200, 500, 1000, 2000 and 5000 mA g^{-1}, respectively. Such high rate performance in the present work is even comparable with previous non-flexible SnS/Carbon composites using heavy current collectors (Table S1). This phenomenon owes to the good charge transfer kinetics

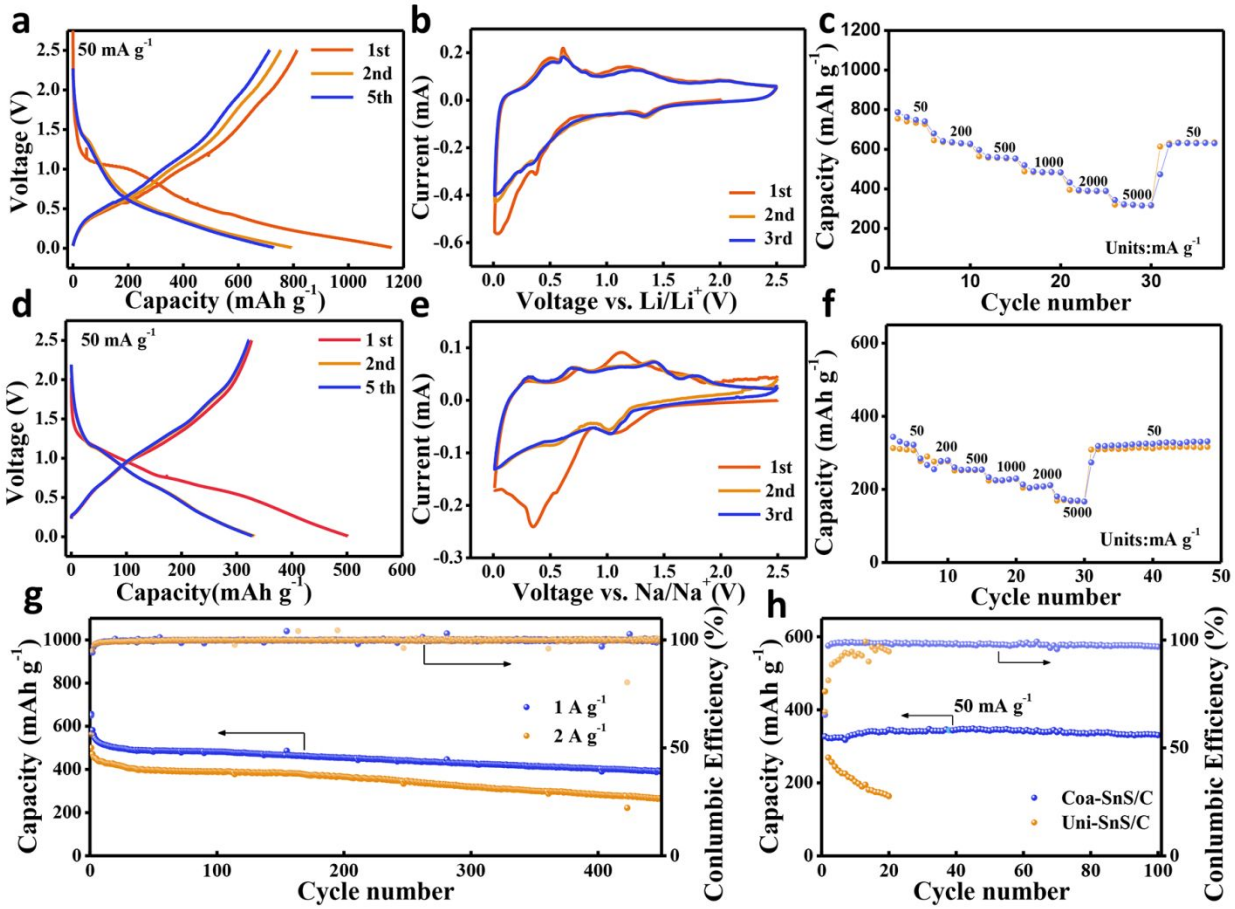

Figure 3. Electrochemical performance for lithium (a-c, g) and sodium (d-f, h) storage: (a, c) Galvanostatic charge/discharge profiles of Coa-SnS/C at 50 mA g^{-1}; (b, e) Cyclic voltammetry curves of Coa-SnS/C at a scan rate of 0.1 mV s^{-1} for the first three cycles; (c, f) Rate capability of Coa-SnS/C; (g) Cycling performance of Coa-SnS/C for lithium storage at 1 A g^{-1} and 2 A g^{-1} separately; (h) Cycling performance of Uni-SnS/C and Coa-SnS/C for sodium storage at 50 mA g^{-1}, respectively.

of the Coa-SnS/C NFs anodes for lithium storage, manifested by EIS analysis, as shown in Figure S4.[52-53, 55] Meanwhile, Figure 3h revealed that Coa-SnS/C exhibits superior cycle stability for lithium storage. The specific charge capacity remains 403.9 mAh g^{-1} after 400 cycles at a current density of 1 A g^{-1}. During cycling, the Coulombic efficiency gradually increases and finally maintains around 99.8% at a current density of 1 and 2 A g^{-1}. Furthermore, after 100 cycles at a current density of 1 A g^{-1}, the superior stability of Coa-SnS/C is observed from the SEM and TEM images (Figure S5).

For sodium storage, the reversible capacity remains 323.3, 276.6, 253.3, 228.6, 210.5 and 166.4 mAh g^{-1}, at the current density of 50, 200, 500, 1000, 2000 and 5000 mA g^{-1}, respectively. Moreover, a high reversible capacity of 330.4 mAh g^{-1} for sodium storage is maintained after 100 stable cycles at a current density of 50 mA g^{-1}. The slight increase in capacity is caused by the activation of Coa-SnS/C during cycling.[51] Notably, the rate performance together with cycling performance of Coa-SnS/C NFs for sodium storage is also comparable among other reported SnS/Carbon composites (Table S2). For comparison, the charge/discharge cycling performance of Uni-SnS/C is investigated in terms of sodium storage at a current density of 50 mA g^{-1}. The reversible capacity only remains 163.4 mAh g^{-1} after 20 cycles even though the first discharge/charge capacities reach 679.6/439 mAh g^{-1}. This phenomenon is attributed to the exposure of SnS nanoparticles on the surface of Uni-SnS/C, where more contact with electrolyte accelerates the conversion and alloying reaction. However, the pulverization caused by large volume change during sodiation/desodiation, which is effectively buffered by carbon matrix in Coa-SnS/C, inevitably leads to serious capacity loss.

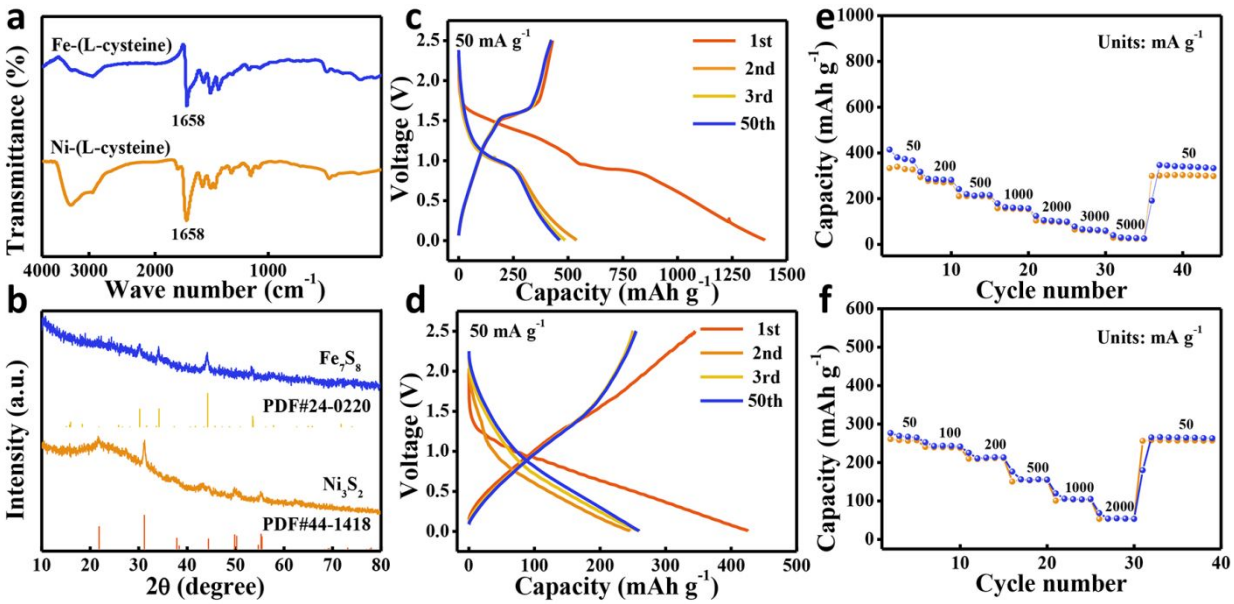

Figure 4. (a) The FT-IR spectra of corresponding precursors of Ni_3S_2/C fibers and Fe_7S_8/C fibers without adding PVP; (b) XRD patterns of Ni_3S_2/C fibers and Fe_7S_8/C fibers; The standard reflections of Ni_3S_2 (JCPDS No. 44-1418) and Fe_7S_8 (JCPDS No. 24-0220) are displayed; (c-d) Galvanostatic charge/discharge profiles of Ni_3S_2/C fibers (c) and Fe_7S_8/C fibers (d) at 50mA g^{-1}, respectively; (e, f) Rate capability of Ni_3S_2/C fibers (e) and Fe_7S_8/C fibers (f), respectively.

From all the above, Coa-SnS/C fabricated via coaxial electrospinning method exhibit the superior electrochemical performance for both lithium and sodium storage. Further considering the freestanding and flexible characteristics, Coa-SnS/C show a favorable prospect not only in anodes of LIBs and SIBs with high performance but also in light-weight and flexible electrodes.

Significantly, this facile method based on the formation of chelate complexes between L-cysteine and metal cations via the coaxial electrospinning method is universally applicable. We have successfully fabricated a series of flexible metal sulfides@carbon fibers and applied these materials as anodes of SIBs. For instances, Ni_3S_2/C fibers and Fe_7S_8/C fibers are obtained by adopting this method under the same condition except for the corresponding metal precursors.

The FT-IR spectra (**Figure 4**a) of mixed solutions containing $NiCl_2$ or $FeCl_2$, and L-cysteine have the same characteristics as that of Coa-SnS/C, demonstrating the identical formation mechanism for these metal sulfides@carbon composites. The representative XRD patterns further reveal the formation of Ni_3S_2 (JCPDS No. 44-1418) and Fe_7S_8 (JCPDS No. 24-0220) while the SEM images illustrate their fibrous morphology. Moreover, such metal sulfides@carbon fibers all exhibit high reversible capacities, good cycling performance and favorable rate performance in terms of sodium storage. Reversible capacities for Ni_3S_2/C fibers and Fe_7S_8/C fibers remain 421.4 and 251.1 mAh g^{-1} after 50 cycles, respectively (Figure 4c-d). When Ni_3S_2/C fibers was discharged and charged at a rate of 200, 500, 1000, 2000, 3000 and 5000 mA g^{-1}, a reversible capacity of 278.0, 210.3, 155.7, 99.4, 61.4 and 26.4 mAh g^{-1} is achieved (Figure 4e). For Fe_7S_8/C fibers, as shown in Figure 4f, the reversible capacity is 260.8, 239.0, 210.4, 153.9, 103.4 and 53.7 mAh g^{-1} under the current density of 50, 100, 200, 500, 1000 and 2000 mA g^{-1}, respectively.

4. Conclusions

A facile and universal strategy to fabricate freestanding and flexible metal sulfides@carbon fibers via a coaxial electrospinning method has been demonstrated. The key to prepare metal sulfides is the formation of bonds between metal cations and R-SH of L-cysteine. Coa-SnS/C is taken as an example to further explore the morphology, structure and electrochemical performance. SnS nanoparticles are uniformly embedded in the continuous and interwoven carbon fibers, to provide fast electron transport pathways and buffer the large volume change during lithium/sodium insertion/extraction. Such freestanding Coa-SnS/C composite exhibits a high reversible capacity, superior cycling stability and excellent rate capability for both lithium

and sodium storage. Moreover, this facile but versatile fabrication strategy can be easily extended to a series of metal sulfides, such as Ni_3S_2/C fibers and Fe_7S_8/C fibers. The proposed strategy might pave the way for fabricating flexible energy storage devices as well as exploring metal sulfide anodes of LIBs/SIBs with excellent electrochemical performance.

ASSOCIATED CONTENT

Supporting Information.

The Supporting Information is available free of charge.

Additional FT-IR, TGA, Raman, EIS and SEM test. (PDF)

AUTHOR INFORMATION

Corresponding Author

* E-mail: Prof. Y. Jiang (yzjiang@zju.edu.cn).

Notes

The authors declare no competing financial interest.

ACKNOWLEDGMENT

This work is supported by National key research and development program (Grant No. 2016YFB0901600), National Natural Science Foundation of China (Grant No. 51722105), Zhejiang Provincial Natural Science Foundation of China (LR18B030001), the Fundamental Research Funds for the Central Universities (2018XZZX002-08), and the Opening Project of CAS Key Laboratory of Materials for Energy Conversion (KF2016002).

REFERENCES

(1) Etacheri, V.; Marom, R.; Elazari, R.; Salitra, G.; Aurbach, D., Challenges in the development of advanced Li-ion batteries: a review. *Energy Environ. Sci.* **2011,** *4*, 3243.

(2) Goodenough, J. B.; Park, K. S., The Li-ion rechargeable battery: a perspective. *J. Am. Chem. Soc.* **2013,** *135*, 1167.

(3) Choi, J. W.; Aurbach, D., Promise and reality of post-lithium-ion batteries with high energy densities. *Nat. Rev. Mater.* **2016,** *1, 16013*.

(4) Zhang, S.; Gu, H.; Pan, H.; Yang, S.; Du, W.; Li, X.; Gao, M.; Liu, Y.; Zhu, M.; Ouyang, L.; Jian, D.; Pan, F., A Novel Strategy to Suppress Capacity and Voltage Fading of Li- and Mn-Rich Layered Oxide Cathode Material for Lithium-Ion Batteries. *Adv. Energy Mater.* **2017,** *7*, 1601066.

(5) Liu, Y.; Pan, H.; Gao, M.; Wang, Q., Advanced hydrogen storage alloys for Ni/MH rechargeable batteries. *J. Mater. Chem.* **2011,** *21*, 4743.

(6) Hwang, J.-Y.; Myung, S.-T.; Sun, Y.-K., Sodium-ion batteries: present and future. *Chem. Soc. Rev.* **2017,** *46*, 3529.

(7) Eftekhari, A.; Kim, D.-W., Sodium-ion batteries: New opportunities beyond energy storage by lithium. *J. Power Sources* **2018,** *395*, 336.

(8) Chayambuka, K.; Mulder, G.; Danilov, D. L.; Notten, P. H. L., Sodium-Ion Battery Materials and Electrochemical Properties Reviewed. *Adv. Energy Mater.* **2018,** *8*, 1800079.

(9) Delmas, C., Sodium and Sodium-Ion Batteries: 50 Years of Research. *Adv. Energy Mater.* **2018,** *8*, 1703137.

(10) Hu, L.; Pasta, M.; Mantia, F. L.; Cui, L.; Jeong, S.; Deshazer, H. D.; Choi, J. W.; Han, S. M.; Cui, Y., Stretchable, porous, and conductive energy textiles. *Nano Lett.* **2010,** *10*, 708.

(11) He, Y. M.; Chen, W. J.; Li, X. D.; Zhang, Z. X.; Fu, J. C.; Zhao, C. H.; Xie, E. Q., Freestanding Three-Dimensional Graphene/MnO_2 Composite Networks As Ultra light and Flexible Supercapacitor Electrodes. *ACS Nano* **2013,** *7*, 174.

(12) Liang, K.; Marcus, K.; Guo, L.; Li, Z.; Zhou, L.; Li, Y.; De Oliveira, S. T.; Orlovskaya, N.; Sohn, Y. H.; Yang, Y., A freestanding NiSx porous film as a binder-free electrode for Mg-ion batteries. *Chem. Commun.* **2017,** *53*, 7608.

(13) Hu, Y.; Ye, D.; Luo, B.; Hu, H.; Zhu, X.; Wang, S.; Li, L.; Peng, S.; Wang, L., A Binder-Free and Free-Standing Cobalt Sulfide@Carbon Nanotube Cathode Material for Aluminum-Ion Batteries. *Adv. Mater.* **2018,** *30*, 1703824.

(14) Wang, Y.; Li, H.; He, P.; Hosono, E.; Zhou, H., Nano active materials for lithium-ion batteries. *Nanoscale* **2010,** *2*, 1294.

(15) Roy, P.; Srivastava, S. K., Nanostructured anode materials for lithium ion batteries. *J. Mater. Chem. A* **2015,** *3*, 2454.

(16) Wang, P.; Gao, M.; Pan, H.; Zhang, J.; Liang, C.; Wang, J.; Zhou, P.; Liu, Y., A facile synthesis of Fe_3O_4/C composite with high cycle stability as anode material for lithium-ion batteries. *J. Power Sources* **2013,** *239*, 466.

(17) Kim, S.-W.; Seo, D.-H.; Ma, X.; Ceder, G.; Kang, K., Electrode Materials for Rechargeable Sodium-Ion Batteries: Potential Alternatives to Current Lithium-Ion Batteries. *Adv. Energy Mater.* **2012,** *2*, 710.

(18) Wen, Y.; He, K.; Zhu, Y.; Han, F.; Xu, Y.; Matsuda, I.; Ishii, Y.; Cumings, J.; Wang, C., Expanded graphite as superior anode for sodium-ion batteries. *Nat. Commun.* **2014,** *5*, 4033.

(19) Kang, H.; Liu, Y.; Cao, K.; Zhao, Y.; Jiao, L.; Wang, Y.; Yuan, H., Update on anode materials for Na-ion batteries. *J. Mater. Chem. A* **2015,** *3*, 17899.

(20) Li, Y.; Hu, Y.-S.; Titirici, M.-M.; Chen, L.; Huang, X., Hard Carbon Microtubes Made from Renewable Cotton as High-Performance Anode Material for Sodium-Ion Batteries. *Adv. Energy Mater.* **2016,** *6*, 61600659.

(21) Luo, W.; Shen, F.; Bommier, C.; Zhu, H.; Ji, X.; Hu, L., Na-Ion Battery Anodes: Materials and Electrochemistry. *Acc. Chem. Res.* **2016,** *49*, 231.

(22) Chen, T.; Ma, Y.; Guo, Q.; Yang, M.; Xia, H., A facile sol–gel route to prepare functional graphene nanosheets anchored with homogeneous cobalt sulfide nanoparticles as superb sodium-ion anodes. *J. Mater. Chem. A* **2017,** *5*, 3179-3185.

(23) Hu, Z.; Liu, Q.; Chou, S. L.; Dou, S. X., Advances and Challenges in Metal Sulfides/Selenides for Next-Generation Rechargeable Sodium-Ion Batteries. *Adv. Mater.* **2017,** *29*, 1700606.

(24) Zhu, Y.; Nie, P.; Shen, L.; Dong, S.; Sheng, Q.; Li, H.; Luo, H.; Zhang, X., High rate capability and superior cycle stability of a flower-like Sb_2S_3 anode for high-capacity sodium ion batteries. *Nanoscale* **2015,** *7*, 3309.

(25) Xie, X.; Ao, Z.; Su, D.; Zhang, J.; Wang, G., MoS_2/Graphene Composite Anodes with Enhanced Performance for Sodium-Ion Batteries: The Role of the Two-Dimensional Heterointerface. *Adv. Funct. Mater.* **2015,** *25*, 1393.

(26) Xiao, Y.; Lee, S. H.; Sun, Y. K. J. A. E. M., The Application of Metal Sulfides in Sodium Ion Batteries. *Adv. Energy Mater.* **2016,** *7*, 1601329.

(27) Lao, M.; Zhang, Y.; Luo, W.; Yan, Q.; Sun, W.; Dou, S. X., Alloy-Based Anode Materials toward Advanced Sodium-Ion Batteries. *Adv. Mater.* **2017,** *29*, 1700622.

(28) Cho, J. S.; Hong, Y. J.; Kang, Y. C., Design and Synthesis of Bubble-Nanorod-Structured Fe_2O_3–Carbon Nanofibers as Advanced Anode Material for Li-Ion Batteries. *ACS Nano* **2015,** *9*, 4026.

(29) Li, X.; Fu, N.; Zou, J.; Zeng, X.; Chen, Y.; Zhou, L.; Lu, W.; Huang, H., Ultrafine Cobalt Sulfide Nanoparticles Encapsulated Hierarchical N-doped Carbon Nanotubes for High-performance Lithium Storage. *Electrochim. Acta* **2017,** *225*, 137.

(30) Zhu, Y.; Han, X.; Xu, Y.; Liu, Y.; Zheng, S.; Xu, K.; Hu, L.; Wang, C., Electrospun Sb/C Fibers for a Stable and Fast Sodium-Ion Battery Anode. *ACS Nano* **2013,** *7*, 6378.

(31) Cho, J. S.; Park, J.-S.; Kang, Y. C., Porous FeS nanofibers with numerous nanovoids obtained by Kirkendall diffusion effect for use as anode materials for sodium-ion batteries. *Nano Research* **2016,** *10*, 897.

(32) Chen, C.; Li, G.; Zhu, J.; Lu, Y.; Jiang, M.; Hu, Y.; Shen, Z.; Zhang, X., In-situ formation of tin-antimony sulfide in nitrogen-sulfur Co-doped carbon nanofibers as high performance anode materials for sodium-ion batteries. *Carbon* **2017,** *120*, 380.

(33) Pan, Y.; Cheng, X.; Huang, Y.; Gong, L.; Zhang, H., CoS2 Nanoparticles Wrapping on Flexible Freestanding Multichannel Carbon Nanofibers with High Performance for Na-Ion Batteries. *ACS Appl. Mater. Interfaces* **2017,** *9*, 35820.

(34) Lu, J.; Nan, C.; Li, L.; Peng, Q.; Li, Y., Flexible SnS nanobelts: Facile synthesis, formation mechanism and application in Li-ion batteries. *Nano Research* **2012,** *6*, 55.

(35) Dokken, K. M.; Parsons, J. G.; McClure, J.; Gardea-Torresdey, J. L., Synthesis and structural analysis of copper(II) cysteine complexes. *Inorg. Chim. Acta* **2009,** *362*, 395.

(36) Novikova, G. V.; Petrov, A. I.; Staloverova, N. A.; Shubin, A. A.; Dergachev, I. D., Complex formation of Sn(II) with L-cysteine: an IR, DTA/TGA and DFT investigation. *Spectrochim Acta A Mol. Biomol. Spectrosc.* **2014,** *122*, 565.

(37) Kumar, N.; Upadhyay, L. S. B., Facile and green synthesis of highly stable l -cysteine functionalized copper nanoparticles. *Appl. Surf. Sci.* **2016,** *385*, 225.

(38) Polivtseva, S.; Acik, I. O.; Katerski, A.; Mere, A.; Mikli, V.; Krunks, M., Tin sulfide films by spray pyrolysis technique using L-cysteine as a novel sulfur source. *physica status solidi (c)* **2016,** *13*, 18.

(39) Pawlukojc, A.; Leciejewicz, J.; Ramirez-Cuesta, A. J.; Nowicka-Scheibe, J., l-Cysteine: Neutron spectroscopy, Raman, IR and ab initio study. *Spectrochim Acta A Mol. Biomol. Spectrosc.* **2005,** *61*, 2474.

(40) Parker, S. F., Assignment of the vibrational spectrum of l-cysteine. *Chem. Phys.* **2013,** *424*, 75.

(41) Wang, L.; Yu, Y.; Chen, P. C.; Zhang, D. W.; Chen, C. H., Electrospinning synthesis of C/Fe_3O_4 composite nanofibers and their application for high performance lithium-ion batteries. *J. Power Sources* **2008,** *183*, 717.

(42) Mendes, L. C.; Rodrigues, R. C.; Silva, E. P., Thermal, structural and morphological assessment of PVP/HA composites. *J. Therm. Anal. Calorim.* **2010,** *101*, 899.

(43) Zhu, S.-C.; Tao, H.-C.; Yang, X.-L.; Zhang, L.-L.; Ni, S.-B., Synthesis of N-doped graphene/SnS composite and its electrochemical properties for lithium ion batteries. *Ionics* **2015,** *21*, 2735.

(44) Xue, P.; Wang, N.; Wang, Y.; Zhang, Y.; Liu, Y.; Tang, B.; Bai, Z.; Dou, S., Nanoconfined SnS in 3D interconnected macroporous carbon as durable anodes for lithium/sodium ion batteries. *Carbon* **2018,** *134*, 222.

(45) Lin, Y.; Gao, M. X.; Zhu, D.; Liu, Y. F.; Pan, H. G., Effects of carbon coating and iron phosphides on the electrochemical properties of $LiFePO_4$/C. *J. Power Sources* **2008,** *184*, 444.

(46) Yan, S.; Abhilash, K. P.; Tang, L.; Yang, M.; Ma, Y.; Xia, Q.; Guo, Q.; Xia, H., Research Advances of Amorphous Metal Oxides in Electrochemical Energy Storage and Conversion. *Small* **2019,** *15*, e1804371.

(47) Zhu, J.; Zhang, X.; Zeng, C.; Liu, A.; Hu, G., Preparation of SnS/graphene nanocomposites from Sn/graphene for superior reversible lithium storage. *Mater. Lett.* **2017,** *209*, 338-341.

(48) Zhao, B.; Wang, Z.; Chen, F.; Yang, Y.; Gao, Y.; Chen, L.; Jiao, Z.; Cheng‡, L.; Jiang, Y., Three-Dimensional Interconnected Spherical Graphene Framework/SnS Nanocomposite for Anode Material with Superior Lithium Storage Performance: Complete Reversibility of Li_2S. *ACS Appl. Mater. Interfaces* **2017,** *9*, 1407.

(49) Zhu, C.; Kopold, P.; Li, W.; van Aken, P. A.; Maier, J.; Yu, Y., A General Strategy to Fabricate Carbon-Coated 3D Porous Interconnected Metal Sulfides: Case Study of SnS/C Nanocomposite for High-Performance Lithium and Sodium Ion Batteries. *Adv. Sci.* **2015,** *2*, 1500200.

(50) Zhou, Y.; Wang, Q.; Zhu, X.; Jiang, F., Three-Dimensional SnS Decorated Carbon Nano-Networks as Anode Materials for Lithium and Sodium Ion Batteries. *Nanomaterials* **2018,** *8*, 135.

(51) Xiong, X.; Yang, C.; Wang, G.; Lin, Y.; Ou, X.; Wang, J.-H.; Zhao, B.; Liu, M.; Lin, Z.; Huang, K., SnS nanoparticles electrostatically anchored on three-dimensional N-doped graphene as an active and durable anode for sodium-ion batteries. *Energy Environ. Sci.* **2017,** *10*, 1757.

(52) Hu, X.; Chen, J.; Zeng, G.; Jia, J.; Cai, P.; Chai, G.; Wen, Z., Robust 3D macroporous structures with SnS nanoparticles decorating nitrogen-doped carbon nanosheet networks for high performance sodium-ion batteries. *J. Mater. Chem. A* **2017,** *5*, 23460.

(53) Chen, S.; Xing, K.; Wen, J.; Wen, M.; Wu, Q.; Cui, Y., Hierarchical assembly and superior sodium storage properties of a sea-sponge structured C/SnS@C nanocomposite. *J. Mater. Chem. A* **2018,** *6*, 7631.

(54) Zhao, X.; Jia, Y.; Liu, Z. H., GO-graphene ink-derived hierarchical 3D-graphene architecture supported Fe3O4 nanodots as high-performance electrodes for lithium/sodium storage and supercapacitors. *J. Colloid Interface Sci.* **2019,** *536*, 463.

(55) Xu, Y.; Zhu, Y.; Liu, Y.; Wang, C., Electrochemical Performance of Porous Carbon/Tin Composite Anodes for Sodium-Ion and Lithium-Ion Batteries. *Adv. Energy Mater.* **2013,** *3*, 128.

A series of freestanding and flexible metal-sulfides/carbon composite electrodes fabricated via a coaxial electrospinning method exhibit high capacity and good cycling stability for both lithium and sodium storage.